Front. Optoelectron. 2016, 9(3): 395–398
DOI 10.1007/s12200-016-0577-4

RESEARCH ARTICLE

Switching dynamics in InP photonic-crystal nanocavity

Yi YU (✉), Evarist PALUSHANI, Mikkel HEUCK, Leif Katsuo OXENLØWE, Kresten YVIND, Jesper MØRK

Department of Photonics Engineering, Technical University of Denmark, 2800 Kgs. Lyngby, Denmark

Abstract In this paper, we presented switching dynamic investigations on an InP photonic-crystal (PhC) nanocavity structure using homodyne pump-probe measurements. The measurements were compared with simulations based on temporal nonlinear coupled mode theory and carrier rate equations for the dynamics of the carrier density governing the cavity properties. The results provide insight into the nonlinear optical processes that govern the dynamics of nanocavities.

Keywords all-optical switching, photonic-crystal (PhC), nanocavity, nonlinear optics

1 Introduction

Photonic-crystal (PhC) employing dispersion tailored waveguides and nanocavities are a promising platform for manipulating light-matter interactions as well as realizing signal processing functionalities, such as ultra-fast and low-energy switching. PhC nanocavity switches have been experimentally demonstrated using carrier effects in different semiconductor materials. An effective carrier lifetime of ~100 ps was obtained using a silicon structure [1], and a decay time of only 15 ps was realized in a GaAs structure [2]. A structure based on InGaAsP material, which carriers were generated through a combination of both linear and two-photon absorption, showed ultra-low energy consumptions and a fast 20 ps switching time window, with a relaxation comprising several different time scales [3,4].

Here we presented pump-probe measurement results of an InP PhC membrane structure with a point defect nanocavity. Thanks to a high quality factor (Q-factor) and small mode volume, this cavity enabled a large switching contrast and fast switching time for low excitation energy. Several different relaxation processes were found in the switching recovery time. The measurements were compared with a numerical model based on nonlinear coupled mode theory to investigate these time constants governing the carrier relaxation. The results provide insight into the nonlinear optical processes that govern the dynamics of nanocavities.

Received December 25, 2015; accepted May 6, 2016

E-mail: yiyu@fotonik.dtu.dk

2 Device

As shown in the scanning electron microscope (SEM) image in the inset in Fig. 1, our PhC structure was an air slab InP membrane consisting of a point-defect H0-type cavity which was formed by shifting two neighboring air holes in opposite directions. The calculated intrinsic Q-factor and the mode volume of the cavity were 25000 and 0.012 μm^3, respectively. The coupling waveguides were standard W1 defect waveguides albeit with the innermost row of holes shifted toward the waveguide center by 42.5 nm to enhance the coupling to the cavity. The detailed fabrication processes have been presented in Refs. [5,6]. The device's resonant wavelength was at 1545.2 nm. The insertion loss (including both propagation and coupling loss) was about −17 dB on resonance.

3 Experimental results and discussion

We used a homodyne pump-probe setup to measure temporal switching dynamics [5]. A short pulse laser (pulsewidth was ~1.5 ps) with a repetition frequency of 1.25 GHz (longer than the free-carrier relaxation time) was employed. Pump and probe signals were generated by band-pass filtering separate parts of a broadband optical source using a multiport optical processor (WaveShaper 4000S). Using a Mach-Zehnder modulator, the probe signal was then chopped at 100 kHz and it was delayed with respect to the pump using a delay line. To avoid pump-probe interactions in the PhC waveguides, a counter-propagating scheme was employed. The states of polarization of both pump and probe signals were adjusted to TE polarization [7] using polarization controllers, and

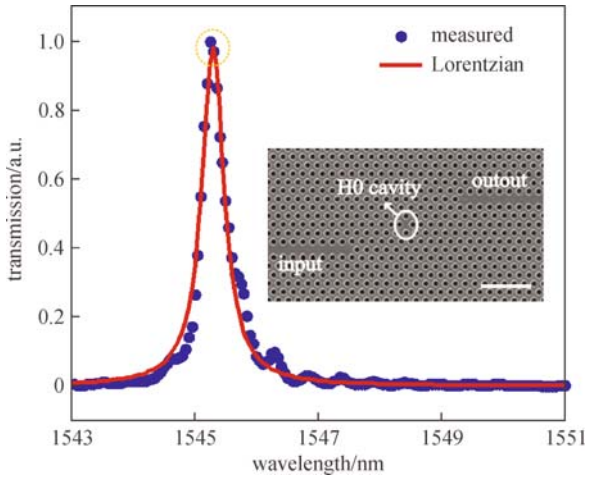

Fig. 1 Transmission spectrum of H0 cavity structure in linear case (blue dots) and theoretical fitting using a Lorentzian function (red curve). The inset shows a SEM image of PhC sample. The scale bar corresponds to 2 μm

they were coupled into and out of the PhC waveguides using lensed single mode fibers. A band-pass filter was used to select the probe signal from the reflected pump. The transmitted probe signal was then detected with a photodiode, amplified, and monitored with a lock-in amplifier. Using power meters and optical spectrum analyzer, the pump and probe signals were monitored, while an infrared camera mounted on a microscope was used to image the far-field scattered light from the top of the sample. We kept the probe power sufficiently weak so as not to cause any unwanted nonlinear effects in the sample. The average probe input power was typically set 7 – 12 dB lower than the average input pump power and the probe-pump detuning was larger than the pump spectral width. For smaller probe power or detuning, interference effects were observed around zero delay. Compared to the heterodyne technique [8], homodyne detection allowed direct measurement of switching contrast and time window, although it required spectral separation of pump and probe signals.

Figure 2 shows the in- and output spectra of the pump for different input powers (without subtracting the coupling loss) and two polarizations (TE or TM). The gray and blue curves represent the cavity linear transmission spectrum and input pump spectrum for reference, both for TE polarization. It can be seen that the output spectrum of the pump expands toward higher frequencies with increasing pump power when TE-polarized, in an agreement with a decrease of the refractive index due to band-filling and free-carrier dispersion of carriers excited by two-photon absorption (TPA). The spectral broadening was observed to increase when the pump was slightly blue detuned with respect to the resonance wavelength. When the pump was TM-polarized as shown in Fig. 2(c), the transmission was, as expected, strongly attenuated due to the absence of a TM photonic band-gap for the PhC, and no clear blueshifts or spectra distortion can be observed.

We also measured the output pump spectra for different modulation rates, i.e., 10 GHz and 625 MHz, as shown in Fig. 3. We estimated the switching energy by subtracting the coupling loss (~7.5 dB) from the pump power at the input fiber. The coupling loss (in dB) was obtained as $(\alpha_{\text{Insertion}} - \alpha_{\text{Cavity}})/2$ under continuous wave excitation, with $\alpha_{\text{Insertion}}$ being the device insertion loss and α_{Cavity} the cavity power transmission at resonance, which depends on the ratio between the total and in-plane Q-factor of the nanocavity. For low repetition rate, as shown in Fig. 3(b), there is a strong spectral peak centered at the input wavelength. This can be explained that a slower repetition rate means the signal has a larger continuous wave component.

Figure 4 shows the measured probe transmission (colored dots) versus pump-probe delay under different pump energies and with two different probe detunings δ, corresponding to switch-on and -off case. We can find a

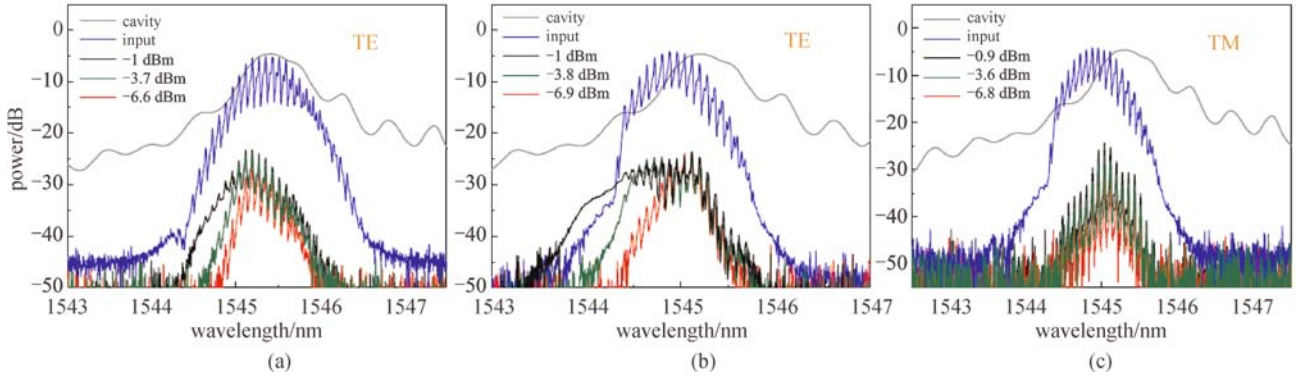

Fig. 2 Input and output pump spectra for different input powers and two polarizations. The probe is absent. (a) The pump is TE-polarized tuned to the cavity resonance; (b) the pump is TE-polarized and is blue detuned by 0.2 nm from the cavity resonance; (c) the pump is TM-polarized and is blue detuned by 0.2 nm from the cavity resonance. The discrete lines located on the spectra is due to modulation

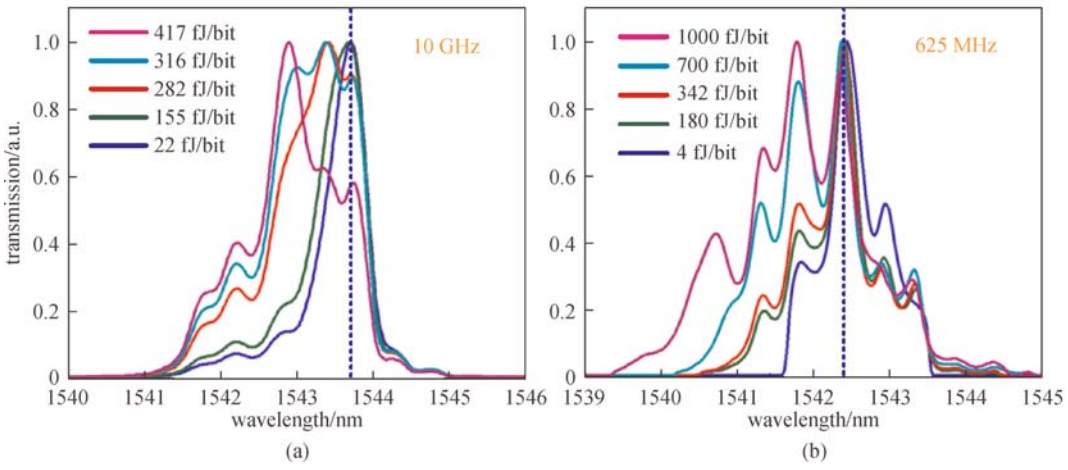

Fig. 3 Normalized output spectra for an input pump signal modulated at (a) 10 GHz and (b) 625 MHz, respectively, with different pulse energies. The input pump signal is tuned to the cavity resonance (blue dashed lines). The spectral curves have been smoothed so the discrete tones due to modulation have been removed

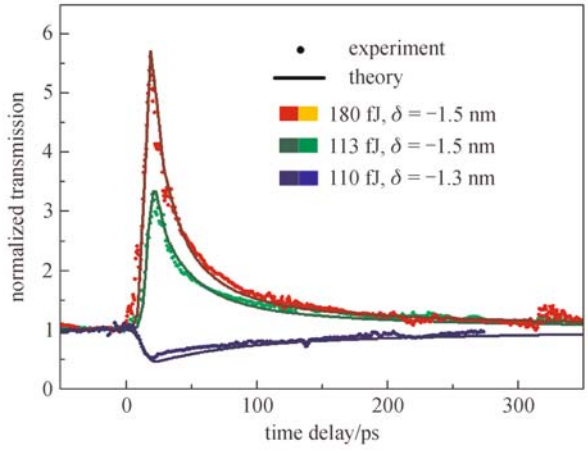

Fig. 4 Measured (dots) and simulated (lines) probe transmission versus pump-probe delay for different pump energies and two probe locations. The transmission was normalized to one when the probe (~9 ps) preceded the pump (~5 –6 ps). The pump wavelength was fixed at 1545 nm. The red and green lines and dots correspond to the switch-on case while the blue line and dot correspond to the switch-off case

good agreement between measurements and simulations (colored lines) using the coupled mode theory model employing three carrier rate equations [5]. In all cases, the transmission recovered in a fast and slow step, similar to the previous findings in Ref. [3]. The time constants do not depend on experimental conditions, but rather intrinsic structural properties. From the comparisons between simulations and experiments, we concluded that thermal effects were negligible at such a low signal repetition rate (the calculated thermal induced resonance red shift was < 0.04 nm) thanks to the high thermal conductivity of InP. For the switch-on case ($\delta < 0$), the switching contrast increased with the pump power. When the strong pump pulse injected into the nanocavity, the probe transmission first reduced due to the combination of TPA loss and instantaneous Kerr effect, which resulted in red shifts of the resonance. This reduction was relatively small and therefore not noticeable in the experiments unless very large pump powers were used. Following the Kerr effect, free carriers were generated through TPA, causing free carrier dispersion, which dominates over the thermo-optic effect, red shifting of the cavity resonance, hence the probe transmission was increased. For the switch-off case ($\delta > 0$), in contrast, the blue-shift of the cavity resonance causes a probe transmission reduction. In Fig. 4, a switching contrast of ~8 dB can be achieved (switch-on case) with an energy of 180 fJ (a lower energy consumption of ~85 fJ was demonstrated for a better switching configuration). According to the simulations, the calculated absorbed energy in the nanocavity was as low as on the order of 20 fJ, showing an efficient light-matter interaction enhancement in the nanocavity.

4 Conclusion

Switching dynamics of InP PhC H0 nanocavities was characterized using a homodyne pump-probe technique, showing fast gating characteristic with large modulation contrast and low energy consumption. The results were compared to simulations based on nonlinear coupled-mode theory, and good agreement was obtained when considering carrier relaxation due to the combined effects of fast carrier diffusion, surface recombination and carrier bulk recombination. Although a short switching window can be achieved by exploiting fast carrier diffusion, the carrier accumulation due to slow recombination was detrimental at high repetition rates.

Acknowledgements The authors acknowledged financial support from Villum Fonden via the NATEC (NAnophotonics for TErabit Communications) Centre and the European Union (COPERNICUS project, FP-ICP-249012).

References

1. Tanabe T, Nishiguchi K, Shinya A, Kuramochi E, Inokawa H, Notomi M, Yamada K, Tsuchizawa T, Watanabe T, Fukuda H, Shinojima H, Itabashi S. Fast all-optical switching using ion-implanted silicon photonic crystal nanocavities. Applied Physics Letters, 2007, 90(3): 031115-1–031115-3
2. Husko C, De Rossi A, Combrié S, Tran Q V, Raineri F, Wong C W. Ultrafast all-optical modulation in GaAs photonic crystal cavities. Applied Physics Letters, 2009, 94(2): 021111-1–021111-3
3. Nozaki K, Tanabe T, Shinya A, Matsuo S, Sato T, Taniyama H, Notomi M. Sub-femtojoule all-optical switching using a photonic-crystal nanocavity. Nature Photonics, 2010, 4(7): 477–483
4. Tanabe T, Notomi M, Mitsugi S, Shinya A, Kuramochi E. Fast bistable all-optical switch and memory on a silicon photonic crystalon-chip. Optics Letters, 2005, 30(19): 2575–2577
5. Yu Y, Palushani E, Heuck M, Kuznetsova N, Kristensen P T, Ek S, Vukovic D, Peucheret C, Oxenløwe L K, Combrié S, de Rossi A, Yvind K, Mørk J. Switching characteristics of an InP photonic crystal nanocavity: experiment and theory. Optics Express, 2013, 21(25): 31047–31061
6. Yu Y, Heuck M, Ek S, Kuznetsova N, Yvind K, Mørk J. Experimental demonstration of a four-port photonic crystal cross-waveguide structure. Applied Physics Letters, 2012, 101(25): 251113-1–251113-4
7. Joannopoulos J D, Johnson S G, Winn J N, Meade R D. Photonic Crystals: Molding the Flow of Light. Princeton: Princeton University, 2008
8. Heuck M, Combrié S, Lehoucq G, Malaguti S, Bellanca G, Trillo S, Kristensen P T, Mørk J, Reithmaier J P, De Rossi A. Heterodyne pump probe measurements of nonlinear dynamics in an indium phosphide photonic crystal cavity. Applied Physics Letters, 2013, 103 (18): 181120-1–181120-4